Journal of Rajasthan Academy of Physical Sciences
ISSN: 0972-6306; URL: http://raops.org.in
Vol.19, No.3&4, July-December, 2020, 167-180

ENTROPY ANALYSIS FOR MIXED CONVECTION IN A POROUS MEDIUM CHANNEL

Paresh Vyas[1], Kusum Yadav[2] and Nupur Srivastava[3]
[1,2]Department of Mathematics, University of Rajasthan, Jaipur, 302004, India
Email: pvyasmaths@gmail.com, kusum.ydv@gmail.com
[3]IIHMR University, Jaipur
Email: nupur2209@gmail.com

Abstract: Entropy generation is analyzed for a steady laminar MHD viscous fluid flow inside a vertical parallel plate porous medium channel. A Cartesian coordinate system is chosen to model the fully developed fluid flow experiencing buoyancy. One wall of the channel is subjected to a convective flux whereas the other wall is kept at uniform temperature. The viscous and Ohmic dissipations are also taken into account. The model simulated numerically provides the distributions for velocity, temperature and entropy number. The effects of pertinent parameters on the entropy number and Bejan number have been reported graphically and discussed.

Key words: MHD, mixed convection, entropy, global entropy, dissipations.

1. Introduction

Experimental and theoretical studies of thermo-fluidics inside channels with or without porous material fillings have been much investigated for applications in building physics, electronic cooling systems, heat exchangers, nuclear reactors, and many more. Besides industrial applications, there exist many natural configurations that can be understood by modeling thermo-fluidics in channels. There is a long list of endeavors in the field which report various aspects such as flow, heat transfer, mixed convection, mass transfer, internal flows and thermally developing flow with variety of wall conditions i.e. uniform wall temperature/ heat flux, axial conduction etc. The central objective of these studies was to extract pertinent information to be employed in industrial and environmental applications. Initially, the thermal aspects in channel/duct flow were treated for clear fluid. On realizing the importance of porous medium as a pertinent heat management tool, thermal characteristics in porous medium channels have also been examined. Shah and London [38] and Kakac and Yener [28] presented a good account on the subject.

Ostrach [37] investigated combined convection in channels with linearly varying wall temperatures. Aung and his co-authors [6, 7, 8, 9] analyzed aspects for channel flow to include developing laminar free convection, fully developed combined convection with flow reversal and mixed convection in ducts with asymmetric wall heat fluxes. Koh and

Colony [29] considered channel flow wherein microstructures of integrating circuits were modeled as "porous material filled vertical channel". Tien and Kuo [41] extended the problem for the case when there was no-slip on the walls. Ingham et al. [27] considered dissipative effects in a parallel channel and addressed both free and forced convection. Banks and Zaturska [10] investigated vertical parallel plane channel where in the flow was due to buoyancy. Al-Hadhrami et al. [5] investigated porous matrix channel experiencing "free-forced convection". Kou and Lu [30] examined laminar mixed convection inside a channel subjected to isoflux and isothermal boundary conditions. Hadim [22] presented a simulation employing Brinkman–Forchheimer model to study vertical porous channel. Chang and Chang [17] offered a numerical study addressing a highly porous composite channel/duct with not fully developed mixed convection. Zanchini [52] examined dissipative mixed convection constrained to Robin condition. In a series of papers, Barletta [11, 12, 13, 14] reported channel flow considering laminar mixed convection, combined forced and free flow with isothermal-isoflux boundary conditions, fully developed flow and viscous heating with prescribed wall heat fluxes, and dual mixed convection. In another series of papers, Nield and his co-authors [33, 34, 35, 36] addressed various flow geometries involving porous channels/circular tube. They investigated thermally developing dissipative forced convection with walls at uniform temperature and with axial conduction, heat flux, isothermal wall etc. Chamkha et al. [16] extended the problem by considering fully developed micropolar free convection fluid flow in a vertical channel. Storesletten and Pop [39] investigated buoyancy effects on flow in a non-isothermal walled channel.

Chen [19] examined mixed convection subjected to constant heat flux occouring in channel. Umavathi et al. [42] treated Brinkman-Forchheimer model for mixed convection in a vertical porous channel and presented numerical and analytical solution. Vyas and Srivastava [50] considered vertically placed channel facilitating oscillatory flow. Adesanya and Makinde [1] studied MHD pulsatile porous channel flow considering the time dependent boundary condition on the heated wall. Ajibade and Bichi [3] investigated variable viscosity impact on transient radiative convection in vertical channel.

Taking a cue that the channel flow configuration is of paramount importance, investigators employed second law of thermodynamics to gauge inherent thermodynamic irreversibility. The central objective was to devise thermodynamic efficiency as per want and the constraints.

Tasnim et al. [40] examined thermodynamic irreversibility encountered in Magneto hydrodynamic flow inside a permeable channel. Mahmud and Fraser [31] extended the study by incorporating dissipative effects. Hooman and Gurgenchi [24] studied entropy generation for temperature-dependent viscosity fluid flow inside a rectangular cross-section and the findings were later utilized by Hooman et al. [25] for entropy generation minimization. Hooman et al. [26] performed entropy analysis for forced convection in a channel. They considered two cases viz. (i) isoflux walls and (ii) isothermal walls. Chauhan and Kumar [18] analyzed entropy inside a composite channel facilitating compressible flow. Das et al. [20] explored entropy generation in a MHD pseudo-plastic

nano-fluid flow inside a porous channel subjected to convective heating. Vyas and his coworkers [43, 48, 49, 45, 47, 51, 46] discussed entropy generation in numerous configurations. Eegunjobi and Makinde [21] numerically analyzed Hall effects on entropy generation in a rotating channel. Hassan et al. [23] examined couple stress flow in a vertical channel. Makinde and Tshehla [32] studied irreversibility in channel flow of cu-water nano-fluid in the presence of suction and injection at the walls. Adesanya et al. [2] studied entropy produced in couple stress fluid flow experiencing exothermic process. Ajibade and Onoja [4] studied irreversibility for convection in a vertical porous channel.

This paper presents entropy analysis in dissipative magnetohydrodynamic flow inside a vertical channel. The configuration comprises a channel containing porous material fully saturated with the fluid and the respective channel walls are constrained to convective flux and constant temperature. The governing boundary value problem has been treated numerically by finite difference scheme. A parametric study unfolds the impact on the entropy production. The set up considered here is an extension of the study by Vyas and Ranjan [44] wherein they had restricted their analysis to transport of energy only.

2. Formulation of the Problem

A steady laminar MHD fully developed flow of a viscous fluid in an infinite porous vertical channel is considered. A Cartesian coordinate system is chosen (refer Figure 1). The vertical channel consists of parallel plates distant 'L' apart. The respective channel walls are subjected to a convective flux and a constant temperature. The set up us exposed to a magnetic field of uniform strength B.

Following Barletta and Zanchini [15], we take characteristic temperature $T_0^* = \frac{\left(T_w^* + T_a^*\right)}{2}$), where T_a^* is the reference temperature.

The BVP for the set up can thus be modeled mathematically as follows:

$$\nu\frac{d^2u^*}{dy^{*2}} + g\beta\left(T^* - T_o^*\right) - \frac{1}{\rho}\frac{dp^*}{dx^*} - \frac{\nu u^*}{k^*} - \frac{\sigma B^2 u^*}{\rho} = 0 \tag{1}$$

$$\kappa\frac{d^2T^*}{dy^{*2}} + \mu\left(\frac{du^*}{dy^*}\right)^2 + \frac{\mu u^{*2}}{k^*} + \sigma B^2 u^{*2} = 0 \tag{2}$$

with the end conditions:

$$y^* = 0 : u^* = 0,\ \kappa\frac{\partial T^*}{\partial y^*} + h_a\left(T_a - T^*\right) = 0 \tag{3}$$

$$y^* = L : u^* = 0, T^* = T_w \tag{4}$$

where μ is the viscosity, $\frac{dp^*}{dx^*}$ is the applied pressure gradient, k^* is the permeability of the porous medium, h_a is the convective heat coefficient, κ is the thermal conductivity, σ is the electric conductivity and ρ is the fluid density.

We prescribe,

$$\left(\kappa \frac{\partial T^*}{\partial y^*}\right)_{y^*=0} + h_a\left(T_a - T^*\right)_{y^*=0} = 0 \tag{5}$$

The equation

$$u_0^* = \frac{1}{L}\int_0^L u^*\left(y^*\right)\, dy^* \tag{6}$$

accounts for the mass flux conservation.

We introduce the following non dimensional quantities:

$$y = \frac{y^*}{L},\ u = \frac{u^*}{u_0^*},\ \theta = \frac{T^* - T_0}{T_w - T_0},\ p = \frac{L^2}{\rho\nu^2}p^*,\ x = \frac{x^* Re}{L} \text{ and } Re = \frac{u_0^* L}{\nu} \tag{7}$$

where Re is the Reynolds number. On using (7), the system of governing equations along with the mass conservation equation (6) is transformed to the following set of non-dimensional equations

$$\frac{d^2u}{dy^2} + \lambda\theta - P - \left(\frac{1}{k} + M^2\right)u = 0 \tag{8}$$

$$\frac{d^2\theta}{dy^2} + Br\left[\left(\frac{du}{dy}\right)^2 + \left(\frac{1}{k} + M^2\right)u^2\right] = 0 \tag{9}$$

with the boundary conditions:

$$y = 0 :\ u = 0,\ \theta'(y) = Bi(1 + \theta(y)) \tag{10}$$

$$y = 1 :\ u = 0,\ \ \theta = 1 \tag{11}$$

and $\int_0^1 u(y)\, dy = 1$ (12)

Where, $\lambda = \frac{Gr}{Re} = \frac{g\beta(T_\omega - T_0)L^2}{\nu U_0}$ is the mixed convection parameter, $P = \frac{dp}{dx}$ is the pressure gradient , $M = \sqrt{\frac{\sigma B^2 L^2}{\rho \nu}}$ is the Hartmann number, $Bi = \frac{h_a L}{\kappa}$ is the Biot number $k = \frac{k^*}{L^2}$ is the permeability parameter and $Br = Pr\,Ec = \frac{\mu u_0^2}{k(T_\omega - T_0)}$ is the Brinkman number.

3. Solution Methodology

The velocity and temperature fields for the configurations under consideration have been obtained in Vyas and Ranjan [44] wherein a rigorous numerical strategy has been used to solve the BVP given by (8) - (11). We followed their code in computing entropy for the setup under consideration. For the sake of brevity, we are not reporting the detailed solution procedure adopted by them; however, we are giving a brief of it. The coupled BVP described by (8) - (11) together with (12) is not amenable to analytic solution hence numerical solution is a natural choice. The problem has been solved by an implicit finite solution strategy together with Gauss Jacobi iteration scheme. Firstly, the domain [0, 1] is discretized by choosing N+2 equi-spaced mesh points

$$y_0 = 0, y_1 = y_0 + h, \ldots, y_i = y_0 + ih, \ldots, y_{N+1} = y_0 + (N+1)h \quad (13)$$

where $h = 1/(N+1)$.

We denote $u(y_i) = u_i$ and $\theta(y_i) = \theta_i$, i=0,1,2,3……N. (14)

The solution methodology involves implicit finite difference scheme with Gauss Jacobi iteration scheme for θ and u. Firstly, the equation (8) is solved for u using finite difference scheme for some initial value of θ in view of the end conditions (10) and (11). Then, with this solution for u, the equation (9) is solved for θ by finite difference method in view of (10) and (11).The process continues until the difference between two consecutive solutions for θ becomes less than for prescribed error tolerance of magnitude 10^{-7}.The finite difference scheme for u is modified to accommodate the integral condition $\int_0^1 u\, dy = 1$ by using Simpson one- third rule for numerical integration. Here, the coefficient matrix is found to be strictly diagonally dominant which is sufficient to ensure that the iterative scheme for θ is convergent for any initial approximation. Actually, the

finite difference scheme used here for the velocity u and the temperature θ pivots on alternate refinement of u and θ both with some initial guess values. First, we start the process for θ yielding an approximate solution for u. With this approximation for u, the temperature θ is further refined. The process is repeated till the end conditions for both u and θ are satisfied to the prescribed error tolerance of order 10^{-7}. The process is continued until $| u^{j+1} - u^{j}| < 10^{-7}$ and $|\theta^{j+1} - \theta^{j}| < 10^{-7}$ criterion is achieved.

4. The Entropy and Global Entropy Analysis

For the problem in hand, S_G that is the local volumetric rate of entropy production is given as

$$S_G = \frac{\kappa}{\left(T_w^* - T_0^*\right)^2}\left(\frac{\partial T}{\partial y^*}\right)^2 + \frac{\mu}{\left(T_w^* - T_0^*\right)}\left(\frac{\partial u^*}{\partial y^*}\right)^2 + \frac{\mu}{\left(T_w^* - T_0^*\right)}\frac{u^2}{k^*} + \frac{\sigma B_0^2 u^{*2}}{\left(T_w^* - T_0^*\right)} \quad (15)$$

The equation (14) underscores that heat transfer, fluid friction, Ohmic and viscous dissipations contribute to entropy. In order to have entropy generation number N_S we define characteristic entropy generation S_{G_0} as follows

$$S_{G_0} = \frac{\kappa}{L^2} \quad (16)$$

Consequently, entropy generation number N_s is obtained as follows

$$N_s = \frac{S}{S_{G_0}} = \left(\frac{d\theta}{dy}\right)^2 + Br\left(\frac{du}{dy}\right)^2 + \left(M^2 + \frac{1}{k}\right)u^2 \quad (17)$$

$$= N_1 + N_2 \quad (18)$$

where $N_1 = \left(\frac{d\theta}{dy}\right)^2$ and $N_2 = Br\left(\frac{du}{dy}\right)^2 + \left(M^2 + \frac{1}{k}\right)u^2$ (19)

stand for heat transfer irreversibility and dissipative irreversibility respectively.

The Bejan number Be is as follows

$$Be = \frac{N_1}{N_1 + N_2} = \frac{\left(\frac{d\theta}{dy}\right)^2}{\left(\frac{d\theta}{dy}\right)^2 + Br\left(\frac{du}{dy}\right)^2 + \left(M^2 + \frac{1}{k}\right)u^2} \quad (20)$$

The global entropy G_{Ns} is computed by integrating the local entropy and on using the Simpson's 1/3 rule, it is found as follows

$$G_S = \frac{1}{3}\left[\left(N_{s_0} + N_{s_{n+1}}\right) + 4\left(N_{s_1} + N_{s_3} + \ldots + N_{s_n}\right) + 2\left(N_{s_2} + N_{s_4} + \ldots + N_{s_{n-1}}\right)\right] \quad (22)$$

5. Results and Discussions

The quantities u, θ and respective gradients computed numerically are employed to compute entropy generation number $N_{S,}$ Bejan number Be and global entropy $G_{Ns.}$ The profiles for the non-dimensional entropy generation number and Bejan number are portrayed for varying parameter values. Before analyzing the figures displaying the effects of different parameters on entropy generation, it is imperative to make certain pertinent remarks so as to understand the physics involved.

The Bejan number Be ($0 \leq Be \leq 1$) is the ratio of heat transfer irreversibility to total entropy generation. Be = 0 signifies the situation where in the thermodynamic irreversibility is due to dissipative effect only and there is no irreversibility due to heat transfer. In contrast to this, when there is no irreversibility due to dissipation, then Be =1 i.e.in this case only temperature gradients contribute to the entropy generation. Furthermore, from the figures we observe that entropy generation number N_s attains minima at various spatial distances in the channel. Its variations in the vicinity of the channel's walls subjected to different thermal conditions are different for different parameter values. As a matter of fact, velocity and temperature gradients are significant near the walls as compared to those in the central region of the channel. In this light, the figures pertaining to entropy have to be peeped into. The figures portraying global entropy against parameters provide wider picture to examine the effects.

The figure 2 shows that entropy generation number N_s increases with increasing values of Hartmann number M in the large part of the channel except the region close to the isothermal wall where the trend is reversed. The figure 3 reveals the impact of Hartmann number M on Bejan number Be. We see that Bejan number Be decays with the increasing values of Hartmann number M. The figure 4 shows that entropy generation N_s increases with the increasing values of the Biot number Bi. The figure 5 exhibits that Bejan number Be decays near the left wall and rises near the right wall of the channel with the rise in values of the Biot number Bi. The figure 6 displays that the entropy generation number N_s increases with the increasing values of Brinkman number Br. It attains minima for respective values of Br whilst recording peaks also somewhere in the middle of the channel. The figure 7 depicts that Bejan number decays with increasing values of Brinkman number Br. The figure 8 shows that the mixed convection parameter λ has significant quantitative effect on entropy generation number $N_{s,}$ prominently in the middle of the channel to the effect that N_s increases with the increasing values of λ. The trend is reversed in the region adjacent to the left wall which is subjected to convective flux. The figure 9 shows that with the increasing values of mixed convection parameter λ, the Bejan number Be increases near the left wall whereas it decreases near the isothermal right wall. From the figure 10 we find that N_s decays in major part of the channel with increasing

values of permeability parameter k except the region adjacent to the isothermal plate. Besides this, we observe that for a given value of k, Ns attain respective minima and maxima at different spatial distances. The figure 11 exhibits that the Bejan number Be increases with increasing values of permeability parameter k. The figure 12 depicts that entropy generation number Ns records an increment with the increasing values of characteristic temperature ratio α; and for a given value of α, Ns attains respective minima and maxima at different spatial distances. The figure 13 depicts that Bejan number Be decreases with increasing values of the characteristic temperature ratio α. The figures 14 – 19 display global entropy versus parameters entering into the problems. The figures 14 & 15 show variations in global entropy number G_{Ns} with respect to the characteristic temperature ratio α wherein it can be seen that the global entropy number increases with increasing values of α, Biot number Bi, mixed convection parameter λ, Brinkman number Br and Hartmann number M. The figure 16 shows variations in global entropy number G_{Ns} with respect to the Br for different values of M and Bi. The figure reveals that G_{Ns} increases with an increase in M, Bi and Br. The figure 17 shows variations in global entropy number G_{Ns} with respect to Br for varying values of k and λ. It is found that G_{Ns} decreases with increasing values of k and λ. The figures 18 and 19 show variations in global entropy number G_{Ns} with respect to the permeability parameter k for different values of λ & α and Br and Bi respectively. It is revealed that G_{Ns} registers an increase with an increase in Br and Bi. We see that the parameters have unequivocal impact on entropy generation and the information may be a launching pad for entropy generation minimization as a future course of endeavour.

6. Conclusions

An entropy analysis for mixed convective flow in a channel was detailed out. Plots for local entropy, global entropy and Bejan number were sketched. It was observed that the quantities of interest respond qualitatively and quantitatively to the parameters entering into the problem. The study offers a basis for future explorations where such configuration may be a part of larger system. The key findings of the study are-

1. The entropy generation number N_s attains minima at various spatial distances in the channel.
2. The global entropy number G_{Ns} increases with increasing values of α, Biot number Bi, Brinkman number Br and Hartmann number M where as it decreases with increasing values of permeability parameter k and mixed convection parameter λ.
3. Bejan number Be decays with the increasing values of Hartmann number M, Brinkman number Br and characteristic temperature ratio α whereas it increases with increasing values of permeability parameter k.
4. Bejan number Be decays near the left wall and rises near the right wall of the channel with the rise in values of the Biot number Bi.
5. With an increase in mixed convection parameter λ, the Bejan number Be increases near the left wall where as it decreases near the isothermal right wall.

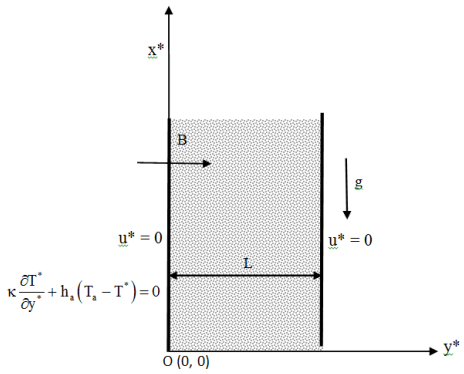

Figure 1: Schematic Diagram

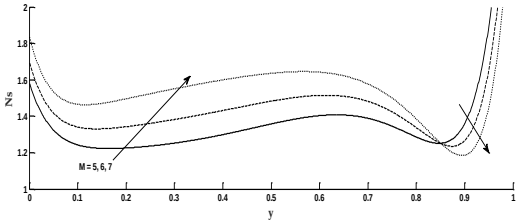

Figure 2: Entropy generation for varying values of M when λ=100, P=-50, Br=0.01, Bi=1, k=1, α=1.

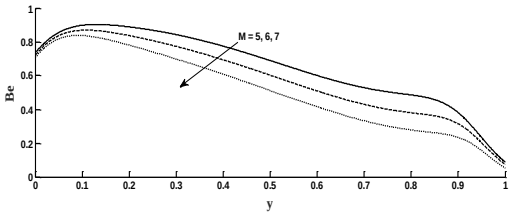

Figure 3: Bejan number for varying values of M when λ=100, P=-50, Br=0.01, Bi=1, k=1, α=1.

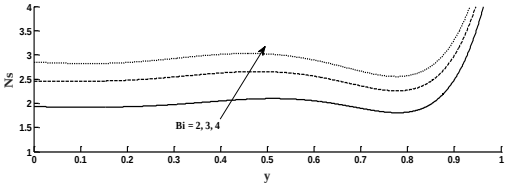

Figure 4: Entropy generation for varying values of Bi when λ=100, P=-50, Br=0.01, M=2, k=1, α=1.

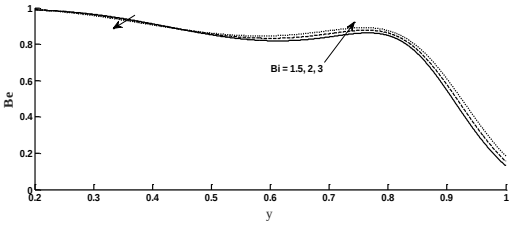

Figure 5: Bejan number for varying values of Bi when λ=100, P=-50, Br=0.01, M=2, k=1, α=1.

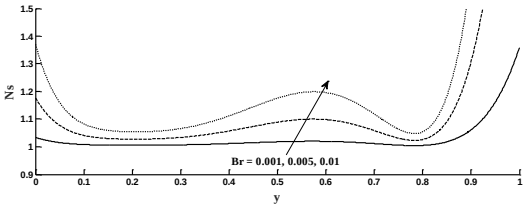

Figure 6: Entropy generation for varying values of Br when λ=100, P=-50, M=2, Bi=1, k=1, α=1.

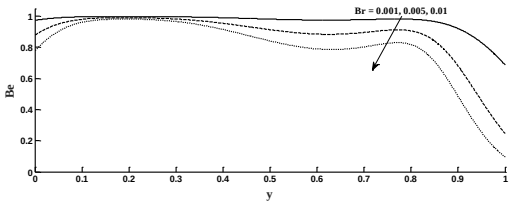

Figure 7: Bejan number for varying values of Br when λ=100, P=-50, M=2, Bi=1, k=1, α=1.

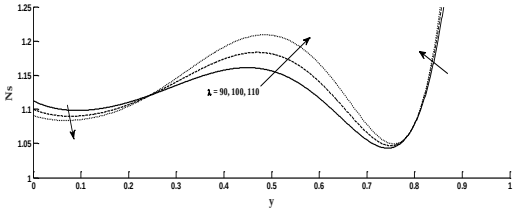

Figure 8: Entropy generation for varying values of λ when P=-3, Br=0.01, M=2, Bi=1, k=1, α=1.

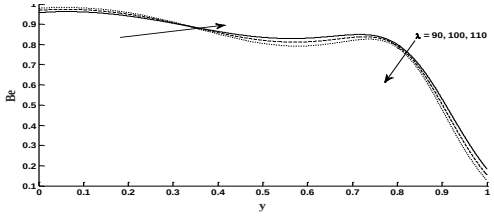

Figure 9: Bejan number for varying values of λ when P=-3, Br=0.01, M=2, Bi=1, k=1, α=1.

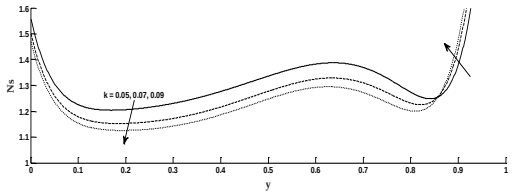

Figure 10: Entropy generation for varying values of k when λ=100, P=-50, Br=0.01, M=2, Bi=1, α=1.

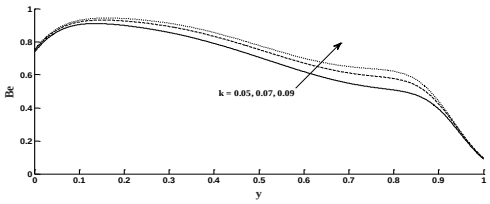

Figure 11: Bejan number for varying values of k when λ=100, P=-50, Br=0.01, M=2, Bi=1, α=1.

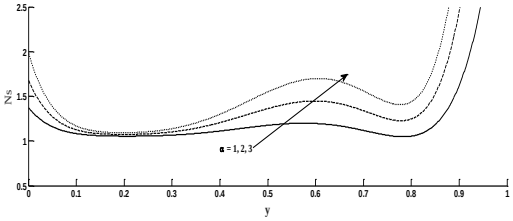

Figure 12: Entropy generation number for varying values of α when λ=100, P=-50, Br=0.01, M=2, Bi=1, k=1.

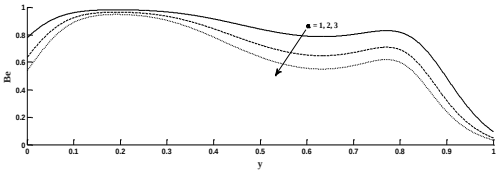

Figure 13: Bejan number for varying values of α when λ=100, P=-50, Br=0.01, M=2, Bi=1, k=1.

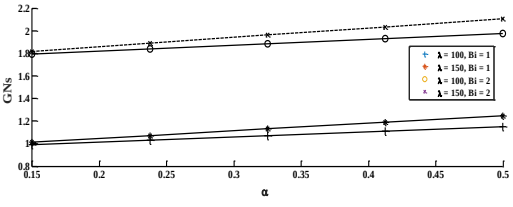

Figure 14: Global entropy generation rate as a function of α for values of λ and Bi, when Br=0.01, M=2, P=-100, Bi=1 and k=1.

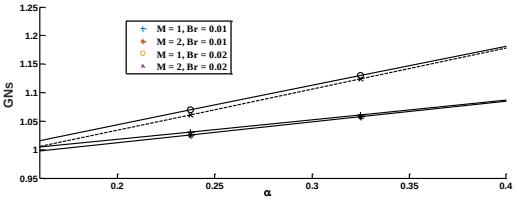

Figure 15: Global entropy generation rate as a function of α for values of M and Br, when Bi=1, λ=100, P=-50, Bi=1 and k=1.

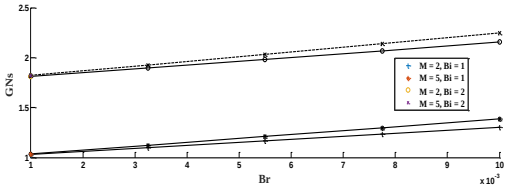

Figure 16: Global entropy generation rate as a function of Br for values of M and Bi, when α=1, λ=100, P=-50, Bi=1 and k=1.

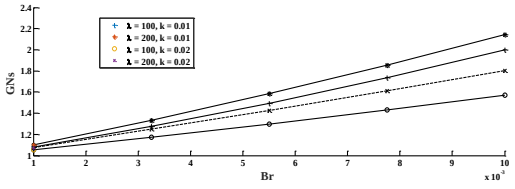

Figure 17: Global generation entropy rate as a function of Br for values of λ and k, when M=2, α=1, P=-50 and Bi=1.

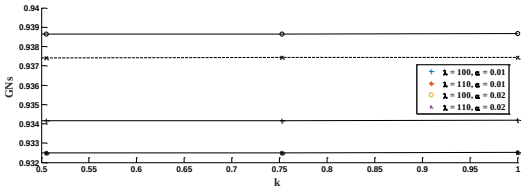

Figure 18: Global entropy generation rate as a function of k for values of λ and α, when M=2, Br=0.01, P=-50 and Bi=1.

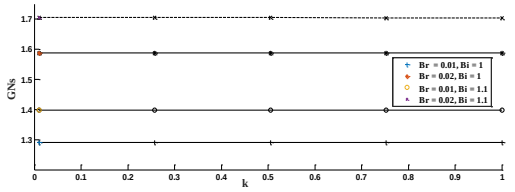

Figure 19: Global entropy generation rate as a function of k for values of Br and Bi, when M=2, Br=0.01, P=-50 and α=1.

Acknowledgements: The authors are thankful to the learned referee for valuable comments and suggestions.

References

[1] Adesanya, S.O. and Makinde, O.D. (2014). MHD oscillatory slip flow and heat transfer in a channel filled with porous media, UPB Sci. Bull. Ser. A, **76** (1), 197-204.

[2] Adesanya, S.O., Falade, J.A., Ukaegbu, J.C. and Lebelo, R.S. (2017). Thermodynamics analysis for a reacting couple stress fluid flow through a vertical channel, Int. J. Pure and Appl. Math. **114**, 419-434.

[3] Ajibade, A.O. and Bichi, Y.A. (2018). Unsteady natural convection flow through a vertical channel: due to the combined effects of variable viscosity and thermal radiation, J. of Appl. and Comp. Mathe. DOI: 10.4172/2168-9679.1000403.

[4] Ajibade, A.O. and Onoja, T.U. (2017). Entropy generation and irreversibility distribution due to steady mixed convection flow in a vertical porous channel, Int. J. of Heat and Tech. **35**, 433-446.

[5] Al-Hadhrami, A.K., Elliott, L. and Ingham, D.B. (2002). Combined free and forced convection in vertical channels of porous media, Transport in Porous Media, **49**, 265-289.

[6] Aung, W. and Worku, G. (1986). Developing flow and flow reversal in a vertical channel with asymmetric wall temperature. J. of Heat Transfer, **108**, 299-304.

[7] Aung, W. and Worku, G. (1986). Theory of fully developed, combined convection including flow reversal, J. of Heat Transfer, **108**, 485-488.

[8] Aung, W., Fletcher, L.S. and Sernas, V. (1972). Development of laminar free convection between vertical plat plates with asymmetric heating, Int. J. Heat Mass Transfer, **15**, 2293-2328.

[9] Aung, W. (1972). Fully developed laminar free convection between vertical parallel plates heated asymmetrically, Int. J. Heat Mass Transfer, **15**, 1577-1580.

[10] Banks, W.H.H. and Zaturska, M.B. (1991). Buoyancy-driven flow between parallel plane vertical walls, J. of Engineering Mathematics, **25**, 375-397.

[11] Barletta, A. (1998). Laminar mixed convection with viscous dissipation in a vertical channel, Int. J. Heat Mass Transfer, **41**, 3501-3513.

[12] Barletta A. (1999). Analysis of combined forced and free flow in a vertical channel with viscous dissipation and isothermal-isoflux boundary conditions, ASME J. Heat Transfer, **121**, 349-356.

[13] Barletta A. (1999). Heat transfer by fully developed flow and viscous heating in a vertical channel with prescribed wall heat fluxes, Int. J. Heat Mass Transfer, **42**, 3873-3885.

[14] Barletta A., Magyari, E. and Keller, B. (2005). Dual mixed convection flows in a vertical channel, Int. J. Heat Mass Transfer, **48**, 4835-4845.

[15] Barletta, A. and Zanchini, E. (1999). On the choice of the reference temperature for fully-developed mixed convection in a vertical channel, Int. J. Heat Mass Transfer, **42**, 3169-3181.

[16] Chamkha, A.J., Grosan, T. and Pop, I. (2003). Fully developed free convection of amicropolar fluid in a vertical channel, Int. J. of Fluid Mechanics Research, **30**, 251-263.

[17] Chang W.J. and Chang W.L. (1996). Mixed convection in a vertical parallel plate channel partially filled with porous media of high permeability, Int. J. Heat Mass Transfer, **39**, 1331-1342.

[18] Chauhan, D.S. and Kumar, V. (2010). Three-dimensional Couette flow in a composite channel partially filled with a porous medium, App. Math. Sci. **4**, 2683-2695.

[19] Chen, Y.C. (2004). Non-Darcy flow stability of mixed convection in a vertical channel filled with a porous medium, Int. J. Heat Mass Transfer, **47**, 1257-1266,

[20] Das, S., Banu, A.S., Jana, R.N. and Makinde, O.D. (2015). Entropy analysis on MHD pseudo-plastic nanofluid flow through a vertical porous channel with convective heating, Alxendria Engineering Journal, **54**, 325-337.

[21] Eegunjobi, A.S. and Makinde, O.D. (2016). Entropy analysis of variable viscosity Hartmann flow through a rotating channel with hall effects, Appl. Math. and Inform. Sci. **10** (4), 1415-1423.

[22] Hadim, A. (1994). Numerical study of non-Darcy mixed convection in a vertical porous channel, J. of Thermophysics and Heat Transfer, **8**, 371-373.

[23] Hassan, A.R., Adesanaya, S.O., Lebelo, R.S. and Falade, J.A. (2017). Irreversibility analysis for a mixed convective flow of a reactive couple stress fluid flow through channel saturated porous materials, Int. J. Heat and Technology, **35**, 633-638.

[24] Hooman, K. and Gurgenci, H. (2007-a). Effects of temperature-dependent viscosity variation on entropy generation, heat, and fluid flow through a porous-saturated duct of rectangular cross-section, Appl. Math. Mech. **28**, 69-78.

[25] Hooman, K., Gurgenci, H. and Merrikh, A. (2007). Heat transfer and entropy generation optimization of forced convection in porous-saturated ducts of rectangular cross-section, Int. J. Heat Mass Transfer, **50** (11-12), 2051-2059.

[26] Hooman, K., Hooman, F. and Mohebpour, S.R. (2008). Entropy generation for forced convection in a porous channel with isoflux or isothermal walls, Int. J. Exergy, **5** (1), 78-96.

[27] Ingham, D.B., Pop, I. and Cheng, P. (1990). Combined free and forced convection in a porous medium between two vertical walls with viscous dissipation, Transport in Porous Media, **5**, 381-398.

[28] Kakac, S. and Yener, Y. (1995). Convective Heat Transfer. CRC Press, Boca Raton, 312.

[29] Koh, J.C.Y., Colony, R. (1986). Heat transfer of microcstructures for integrated circuits, Int. Commun. in Heat and Mass Transfer, **13**, 89-98.

[30] Kou, H.S., Lu, K.L. (1993). Combined boundary and inertia effects for fully developed mixed convection in a vertical channel embedded in porous media, Int. Commun. in Heat and Mass Transfer, **20**, 333-345.

[31] Mahmud, M. and Fraser, R.A. (2005). Flow, thermal, and entropy generation characteristics inside a porous channel with viscous dissipation, Int. J. Thermal Sciences, **44** (1), 21-32.

[32] Makinde, O.D. and Tshehla, M.S. (2017). Irreversibility analysis of mixed convection channel flow of nano-fluid with suction injection, Global J. of Pure and Appl. Math., **13**, 4851- 4867.

[33] Nield, D.A., Kuznetsov A.V. and Xiong M. (2003). Thermally developing forced convection in a porous medium: parallel-plate channel or circular tube with walls at constant heat flux, J. Porous Media, **6**, 203-212.

[34] Nield, D.A., Kuznetsov, A.V. and Xiong, M. (2003). Thermally developing forced convection in a porous medium: parallel plate channel with walls at uniform temperature, with axial conduction and viscous dissipation effects, Int. J. Heat Mass Transfer, **46**, 643-651.

[35] Nield, D.A., Kuznetsov, A.V. and Xiong, M. (2004). Effects of viscous dissipation and flow work on forced convection in a channel filled by a saturated porous medium, Transport Porous Media, **56**, 351-367.

[36] Nield, D.A. (2004). Forced convection in a parallel plate channel with asymmetric heating. Int. J. Heat Mass Transfer, **47**, 5609-5612.

[37] Ostrach, S. (1954). Combined natural- and forced-convection laminar flow and heat transfer of fluid with and without heat sources in channels with linearly varying wall temperatures, NACA TN, 3141.

[38] Shah, R.K. and London, A.L. (1978). Advances in Heat Transfer, Suppl. 1. Academic Press, New York.

[39] Storesletten, L. and Pop, I. (1996). Free convection in a vertical porous layer with walls at non-uniform temperature, Fluid Dyn. Res. **17**, 107-119.

[40] Tasnim, S. H., Mahmud S. and Mamun, M.A.H. (2002). Entropy generation in a porous channel with hydromagnetic effects, Exergy, **2** (4), 300-308.

[41] Tien, C. L. and Kuo, S. M. (1987). Analysis of forced convection in microstructures for electronic system cooling. In Proceedings of the International Symposium on Cooling Technology for Electronic Equipment, Honolulu, Hl, 217-226.

[42] Umavathi, J.C., Kumar, J.P., Chamkha, A.J. and Pop, I. (2005). Mixed convection in a vertical porous channel, Transport Porous Media, **61**, 315-335.

[43] Vyas, P. and Khan, S. (2016). Entropy analysis for MHD dissipative Casson fluid flow in porous medium due to stretching cylinder, Acta Technica, **61**, 299-315.

[44] Vyas, P. and Ranjan, A. (2014). Ph.D thesis entitled "Studies in Magnetohydrodynamic Fluid Flow in the Presence of Permeable Beds" submitted to University of Rajasthan, Jaipur, India.

[45] Vyas, P. and Soni, S. (2016). Entropy analysis for MHD Casson fluid flow in a channel subjected to weakly temperature dependent convection coefficient and hydrodynamic slip, J. of Raj. Acad. of Phys. Sci. **15**, 1-18.

[46] Vyas, P. and Soni, S. (2017). On entropy generation in radiative MHD boundary layer flow with partial slip due to a melting surface stretching in porous medium. J. of Raj. Acad. of Phys. Sci. **16**, 93-111.

[47] Vyas, P. and Soni, S. (2016). On entropy regime for flow and heat transfer over a naturally permeable bed subjected to a variable suction, J. of Raj. Acad. of Phys. Sci. **15**, 299-313.

[48] Vyas, P. and Srivastava, N. (2015). Entropy analysis for magnetohydrodynamic fluid flow in porous medium due to non-isothermal stretching sheet, J. of Raj. Acad. of Phys. Sci. **14**, 323-336.

[49] Vyas, P. and Srivastava, N. (2015). Entropy analysis of generalized MHD couette flow inside a composite duct with asymmetric convective cooling, Arab. J. Sci. and Eng. **40**, 603-614.

[50] Vyas, P. and Srivastava, N. (2013). Oscillatory flow in a vertical channel filled with porous medium with radiation and dissipation, Walailak J. Sci. & Tech. **10** (5), 531-552.

[51] Vyas, P., Srivastava, N. and Soni, S. (2016). Entropy generation analysis for oscillatory flow in a vertical channel filled with porous medium, Int. Confer. On Recent Advances and Innovations in Engineering (ICRAIE), Jaipur, 1-6, 10.1109/ICRAIE.2016.7939542.

[52] Zanchini, E. (1998). Effect of viscous dissipation on mixed convection in a vertical channel with boundary conditions of the third kind, Int. J. Heat Mass Transfer, **41**, 3949-3959.